THE JOURNAL OF PHYSICAL CHEMISTRY B

Article

pubs.acs.org/JPCB

# Linking On-State Memory and Distributed Kinetics in Single Nanocrystal Blinking

Amy A. Cordones,[†] Kenneth L. Knappenberger, Jr.,[‡] and Stephen R. Leone*,[†]

[†]Departments of Chemistry and Physics, University of California and Lawrence Berkeley National Laboratory, Berkeley, California 94720, United States

[‡]Department of Chemistry and Biochemistry, Florida State University, Tallahassee, Florida 32306-4390, United States

Supporting Information

**ABSTRACT:** Memory effects in single nanocrystal fluorescence blinking are investigated as a function of the on-state kinetics for CdSe/ZnS quantum dots and CdSe nanorods. The on-state duration probability distributions for single nanocrystal blinking traces are characterized by an inverse power law, which crosses over to exponential decay for long on-state durations. The correlations of subsequent on-state durations ($R_{log,on}$) are found to decrease for nanocrystals that display earlier crossover times and smaller power law coefficients. Specifically, $R_{log,on}$ increases from 0.14 ± 0.02 to a saturation value of 0.44 ± 0.01 for nanocrystals with average crossover times of ∼100 ms to more than 5.0 s, respectively. The results represent the first link between memory effects and blinking kinetics and are interpreted in the framework of two competing charge trapping mechanisms. A slow fluctuation-based trapping mechanism leads to power-law-distributed on durations and significant memory effects; however, the additional contribution of an ionization-induced trapping pathway is found to induce crossover to exponential decay and decreased memory. Monte Carlo simulations of nanocrystal blinking based on the two trapping mechanisms reproduce the experimental results, suggesting that the power law component and the memory effects correlate with a fluctuation-based mechanism. This effect is found to be universal, occurring for two nanocrystal morphologies and in blinking data measured using a wide range of continuous and pulsed excitation conditions.

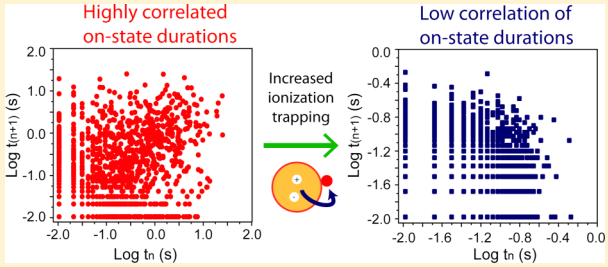


## I. INTRODUCTION

Fluorescence intermittency, or blinking, is observed ubiquitously in single emitters including dye molecules, biological molecules, and nanostructures. Since the original observation of nanocrystal (NC) blinking in CdSe quantum dots,[1] intermittency has been observed from single particles of wide-ranging composition[2−4] and structure, including nanorods[5] and nanowires.[6] The large jumps in fluorescence intensity that characterize the blinking process are observed to occur over multiple time scales, out to hundreds of seconds, and often prove to be detrimental to many potential NC-based applications. A detailed understanding of the origin of the blinking behavior is important to gain better control over the NC fluorescence properties; however, these origins are still not fully understood.

Initially proposed NC blinking mechanisms focused on Auger ionization as the cause of the jumps from the fluorescent on-state to the nonfluorescent off-state.[7] In this case, the NC remains dark due to the nonradiative Auger recombination of subsequent excitons in the charged NC core and becomes fluorescent again upon neutralization. This mechanism, however, is inconsistent with the highly distributed kinetics observed in NC blinking, as probability distributions of the on- and off-state durations were shown to be inverse power law distributed.[8,9] Several recent reports also directly challenge the Auger recombination quenching mechanism of the off-state based on experimental measurement and simulation of the off-state fluorescence quantum yield and decay lifetime.[10−13]

Several recent NC blinking mechanisms that are successful in predicting the distributed kinetics observed in the on- and off-state probability distributions rely on a slowly diffusing coordinate. For example, diffusion in energy of the charge trapping states[9] or of the QD energy levels[14,15] leads to slow fluctuations of the charge transfer rate and therefore distributed trapping kinetics. The slowly diffusing coordinate is often associated with fluctuations in the NC local environment. For example, recent theory work reports energetic diffusion of trap states that are localized in highly mobile ligand species.[16] Conformational changes of surface trapping sites are also predicted to cause fluctuations in the hole trapping rate according to the multiple recombination centers mechanism.[17] These models have all been shown to reproduce the power law on- and off-state probability distributions observed experimentally. Slowly fluctuating degrees of surface charging and charge

**Special Issue:** Paul F. Barbara Memorial Issue

**Received:** April 30, 2012
**Revised:** September 5, 2012
**Published:** September 11, 2012

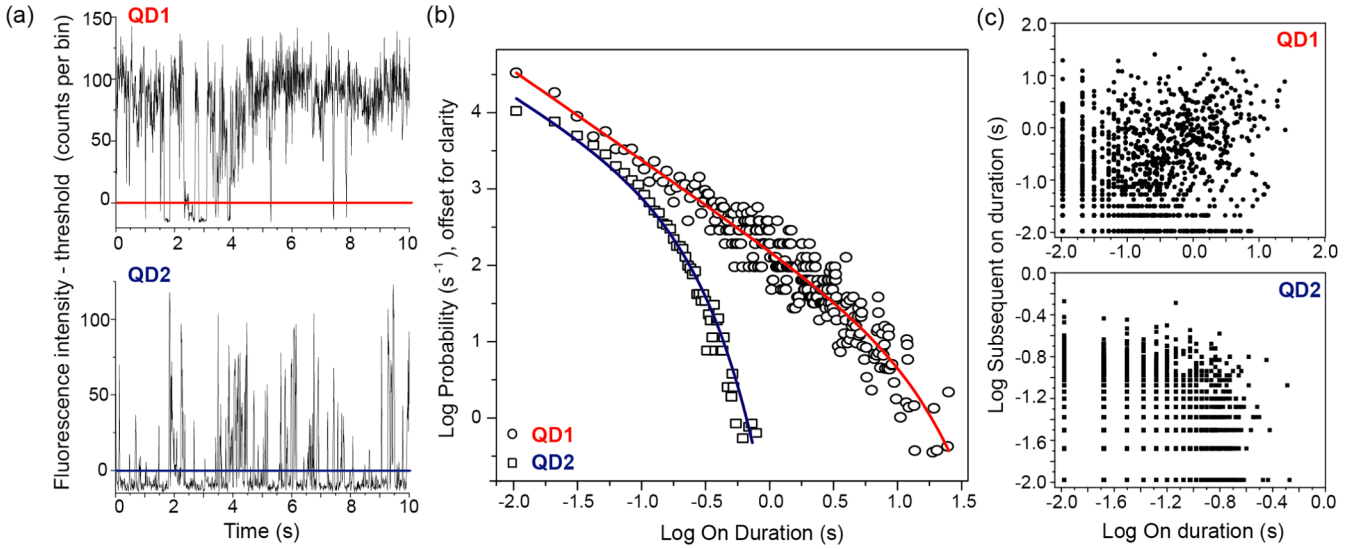


**Figure 1.** Fluorescence blinking data for two single CdSe/ZnS QDs, with pulsed laser excitation at 500 nm. (a) 10 s of blinking is shown for each QD; the threshold separating the on- and off-state is shown. (b) On-state probability distributions for each QD are fit to eq 1. $\tau_c$ = 10.7 ± 1.1 s for QD1 and $\tau_c$ = 0.117 ± 0.015 s for QD2. (c) Scatter plots of subsequent on durations are shown for both QDs. A higher degree of memory is observed in QD1 with $R_{log,on}$ = 0.39, compared to QD2 with $R_{log,on}$ = 0.09.

migration have also been invoked to explain the continuous distribution of emissive states[18] and low off-state quantum yields[10] observed during blinking.

There have been relatively few studies to investigate memory effects in NC blinking.[4,19−21] Although the mechanism is not the same, it has been previously established that the slow conformational changes that cause fluorescence blinking in enzymes lead to correlations in the subsequent on- and subsequent off-state durations.[22] It is natural to apply a similar analysis to NCs, as several NC blinking mechanisms also invoke a slowly fluctuating parameter that determines the on-to-off or off-to-on switching rates. Initial investigations of memory effects in CdSe and InP quantum dots focused on scatter plots of subsequent on (off) events, and no obvious correlations were reported.[4,19] Further studies by Stefani et al. found that, when plotted on a logarithmic scale, correlations are observed in subsequent on (off) events.[20] These correlations were observed to be long-lived and found for on (off) events separated by up to 3−4 s. These results indicate a residual memory in the fluctuations that may be responsible for NC blinking.

The degree of memory for successive on (off) durations was also measured as a function of excitation intensity and local environment.[20] The correlations of subsequent on (off) events were not found to vary with laser power or substrate. Similarly, the power law decay observed for on- and off-state duration probability distributions is usually reported as insensitive to many experimental parameters. The authors cite this similarity and suggest that the memory effects are therefore due to the power law distributed blinking mechanism; however, a direct link between the two has not been experimentally established.

In this work, we examine the link between the degree of memory in the NC blinking traces and the kinetics of the underlying blinking mechanism. We show for the first time a direct correlation between the on duration memory effects and power law blinking statistics. To illustrate this point, a wide range of on-state duration probability distributions are needed and generated from the blinking data of two NC morphologies under various excitation conditions. These distributions are found to truncate from an inverse power law at times ranging from hundreds of milliseconds to tens of seconds, and this truncation is correlated with the degree of memory. Specifically, we observe a decrease in subsequent on duration memory from those NCs with an early truncation time. This result marks the first observation of the correlation of memory effects and blinking statistics and suggests that the power law distributed component and memory effect originate from a similar fluctuation-based mechanism. Furthermore, Monte Carlo simulations are employed to show that additional contributions from an ionization-based trapping mechanism reproduce the experimentally observed decrease in correlation coefficient and truncation time.

## II. EXPERIMENTAL SECTION

The blinking data that comprise this work originate from three different NC samples. Commercial core/shell CdSe/ZnS quantum dots (QD) were purchased from Evident Corporation (ED-C11-tol-0600) and Ocean NanoTech (QSP-600-0050). The lowest energy transition is found to occur at 2.12 eV for both samples by ensemble absorbance measurements, corresponding to a core size of approximately 4 nm.[23] The fluorescence maxima are measured to be 2.05 and 2.08 eV (Evident and Ocean NanoTech, respectively). CdSe nanorods were prepared as described in ref 24. The lowest energy transition is found to occur at 2.35 eV, and the fluorescence maximum occurs at 2.27 eV. All NC samples are deposited on microscope coverslips passivated with *N*-(2-aminoethyl)-3-aminopropyltrimethoxysilane by spin coating or drop-casting to obtain sample densities of less than 0.1 NC/$\mu$m$^2$, as measured from wide-field fluorescence images and atomic force microscopy (AFM).

A home-built confocal fluorescence microscope is used in the epifluorescence configuration to collect single nanocrystal fluorescence time traces. To show the universality of the blinking trends reported here, a variety of excitation and collection configurations are used. Some fluorescence data are collected using a pulsed excitation source of tunable visible wavelength with per pulse excitation intensities covering the single and multiphoton regime, as described in ref 25. In this


dx.doi.org/10.1021/jp3041549 | J. Phys. Chem. B 2013, 117, 4241−4248

configuration, single NC fluorescence is detected by single photon counting avalanche photodiodes (PDM series, MPD). Each detected photon is time-tagged and subsequently binned with 10.5 ms resolution to create fluorescence blinking traces. This detection scheme is also used for CdSe/ZnS quantum dot (QD) data excited with a 405 nm continuous laser. The power density was maintained at 450 W/cm$^2$ for excitation from this source. For the CdSe nanorod data, a 543 nm continuous laser is used in a wide-field configuration, such that several QDs are imaged within the excitation volume. The power density was varied from 100 to 450 W/cm$^2$ for this excitation source. The fluorescence is detected using a charge-coupled device (CCD) camera, and the signal is read to a video capture card. Pixel areas corresponding to individual nanorod fluorescence are selected, and the intensity is integrated over time with a resolution of 33.4 ms. Blinking experiments using all microscope configurations last 10−20 min in duration.

Representative blinking traces (10 s subsections) from two different single CdSe/ZnS quantum dots (QD) are shown in Figure 1a. A threshold value is defined to separate the on- and off-state intensity levels by a method previously described in ref 25. After a threshold is defined, the blinking trace is broken into a series of on- and off-state durations. Probability density distributions for the on-state and off-state durations are calculated according to ref 19 and plotted on a log−log scale (Figure 1b). The off duration distributions are typically well described by an inverse power law, and only under high excitation intensity conditions is a deviation from power law behavior observed.[25] Because the focus of this work is the deviation from power law decay, which only is observed for the off-state in a small subset of high intensity data, the off duration distributions are not considered further. The on-state duration probability distributions are well described by an inverse power law decay that crosses over to exponential for longer on-state durations (Figure 1b).

$$P(\tau_{on}) \propto \tau_{on}^{-\alpha_{on}} e^{-\tau_{on}/\tau_c} \quad (1)$$

The log−log data are binned along the $x$-axis and averaged to produce a data set that is equally distributed along the $x$-axis (this procedure equally weights all regions of the log−log data set). The binned data is fit to eq 1 to extract the power law coefficient, $\alpha_{on}$, and the crossover time, $\tau_c$. which marks the onset of exponential truncation. Note the large difference in $\tau_c$ values in Figure 1b, which are illustrative of the large range of values measured here, spanning two decades in time, as discussed further below.

On-state memory effects, or correlations in subsequent on-state or off-state durations, are also analyzed. Scatter plots of duration versus subsequent duration are used here to provide visualization of such correlations, consistent with previous work.[19,20] Figure 1c shows two examples of scatter plots to examine correlations of subsequent on-state durations. A linear correlation coefficient is calculated to quantify the degree of correlation in the scatter plots. The correlation coefficient, $R$, is calculated as

$$R = \frac{\sum_n (\tau_n - \overline{\tau_n})(\tau_{n+1} - \overline{\tau_{n+1}})}{\sqrt{\sum_n (\tau_n - \overline{\tau_n})^2}\sqrt{\sum_n (\tau_{n+1} - \overline{\tau_{n+1}})^2}} \quad (2)$$

where $\tau_n$ is the duration of the $n$th on-state event and $\overline{\tau_n}$ is the average on duration. Highly correlated data form linear scatter plots with a slope of 1 and $R = 1$, while anticorrelated data are linear with a slope of −1 and $R = -1$. Completely uncorrelated data result in $R = 0$. It has been shown previously that the correlation between subsequent on-state (or off-state) durations becomes more evident when examined on a log−log scale.[20] $R_{log}$ is calculated by replacing each $\tau$ value of eq 2 with $\log(\tau)$, which results in a heavier emphasis of the correlation of short duration events. Again, the scatter plots of $\log(\tau_n)$ versus $\log(\tau_{n+1})$ for the two QDs in Figure 1c illustrate the large range of $R_{log,on}$ values reported here.

## III. RESULTS

This work considers the link between power law blinking and subsequent duration memory effects. The full range of blinking behavior reported here is first illustrated on the basis of two individual quantum dots (QD) in Figure 1. It is apparent from examination of the blinking traces in Figure 1a that QD2 exhibits considerably faster switching rates between the on and off states compared to QD1. This trend is quantified by the probability distributions of on-state durations (Figure 1b), which indicate on durations more than 45 times longer are observed in QD1 compared to QD2. The probability distribution for QD1 is well fit to a power law distribution with a crossover to exponential decay ($\tau_c$) at 10.7 ± 1.1 s. The probability distribution for QD2, however, is more highly exponential and has a crossover time of 0.117 ± 0.015 s.

On-state duration memory is also compared for QD1 and QD2, and scatter plots of subsequent on-state durations are shown in Figure 1c. A high degree of correlation is observed for QD1, resulting in $R_{log,on} = 0.39$. This value is consistent with a previous report by Stefani et al. for ZnCdSe QDs on glass, which have an average $R_{log,on} = 0.37 \pm 0.06$.[20] A much smaller degree of correlation is observed for the subsequent on durations of QD2, resulting in $R_{log,on} = 0.09$. The two examples presented in Figure 1 illustrate a general trend reported here that NCs displaying blinking behavior dominated by an exponentially distributed process have less correlated subsequent on-state durations.

This link is further explored for a much larger set of blinking data. Figure 2a shows the relationship between the on-state memory and power law distributed blinking by plotting $R_{log,on}$ as a function of $\tau_c$ for all NCs measured. This data set includes blinking traces from 220 NCs, and $\tau_c$ is plotted on a log scale to show more clearly the full range of values measured. A large range of $\tau_c$ values are necessary to observe the reported $R_{log,on}$ dependence, and a variety of excitation conditions are used to produce such a range. Two NC morphologies are used (CdSe/ZnS QDs and CdSe nanorods), and both pulsed and continuous laser excitation of varying intensity and wavelength are employed. In comparing the two NC morphologies measured under continuous excitation, we note that overall shorter $\tau_c$ values are measured for the elongated nanorods, which have a larger surface area and most likely larger number of surface trapping sites. However, the nanorod samples yield the same trend of decreasing $R_{log,on}$ with decreasing $\tau_c$ as the spherical quantum dots. The consistency of this data taken under such varied conditions highlights the universality of the results presented here.

The data from Figure 2a are binned by crossover time and averaged along linear $x$- and $y$-axes, as presented in Figure 2b. The qualitative trend shown for the two QDs in Figure 1 is observed for the large data set. From the averaged plot in Figure 2b, $R_{log,on}$ is observed to decrease from 0.438 ± 0.009 for NCs with $\tau_c > 5.0$ s to 0.14 ± 0.02 for NCs with an average $\tau_c$ = 103 ± 20 ms. Thus, there is a strong correlation between a high


dx.doi.org/10.1021/jp3041549 | J. Phys. Chem. B 2013, 117, 4241−4248

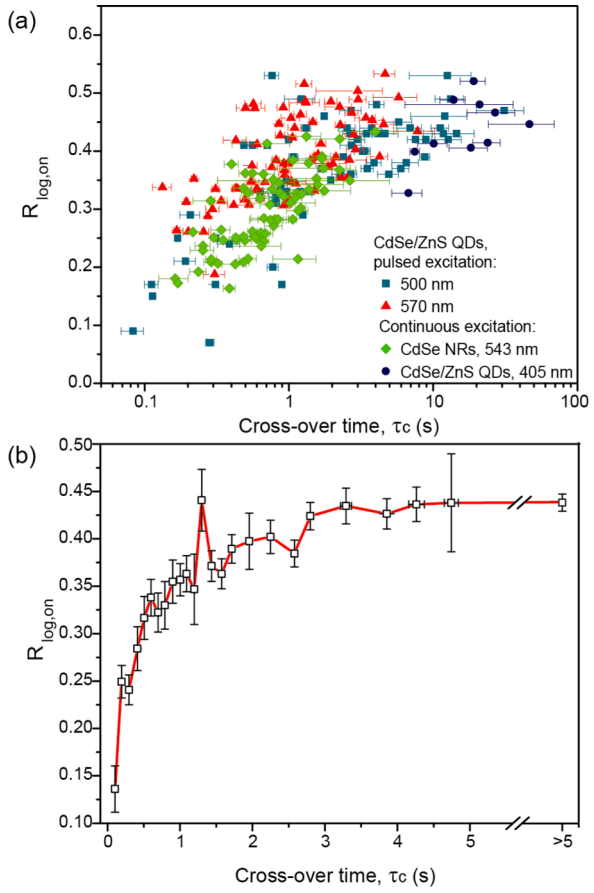


**Figure 2.** The correlation of $R_{log,on}$ and $\tau_c$ for all NCs investigated. (a) Data from 220 NCs are plotted together, with NC composition, morphology, and excitation conditions indicated on the plot. $\tau_c$ is plotted on a logarithmic scale. (b) The data plotted in part a are binned by $\tau_c$ and averaged along the linear *x*- and *y*-axes. The range of the error bars is 2 standard deviations of $\tau_c$ and 2 standard deviations of the mean of $R_{log,on}$. All data with $\tau_c \geq 5.0$ s are averaged together, as $R_{log,on}$ has already saturated.

degree of on-state memory and a large contribution of power law distributed blinking.

Before physical mechanisms are considered to account for the correlation of on-state memory and crossover time, we first acknowledge that a smaller crossover time also indicates shorter on-state durations overall. In an attempt to address how the memory changes for blinking traces with shorter on-state durations, but without involving the exponential truncation, a small subset of CdSe QD blinking traces with pure power law on-state duration probability distributions are analyzed. $R_{log,on}$ is found not to correlate with the maximum on-state duration observed for each QD. Additionally, $R_{log,on}$ is calculated for individual QDs from this data after removing all sets of subsequent events involving durations longer than 1.0 s. The removal of long on-state durations does decrease $R_{log,on}$ but not by a constant factor from one QD to another. This analysis suggests that the decreased number of long on-state durations for the small $\tau_c$ data may contribute to the decrease in $R_{log,on}$. In the remaining discussion, multiple physical processes leading to smaller $\tau_c$ values and, therefore, less long on-state durations are considered. While all simulated blinking mechanisms reproduce the qualitative trend of decreasing $R_{log,on}$ with decreasing $\tau_c$, they are dissimilar in the saturation behavior and magnitude of change. Were the reported trend due to a purely mathematic effect, all cases with the same $\tau_c$ value would yield the same decrease in $R_{log,on}$. We do not dismiss the contribution of some purely mathematical effect behind the decrease in memory; however, we find the mechanisms tested here to vary sufficiently to provide insight into the physical processes behind blinking.

In the remaining discussion, we consider only physical processes capable of reproducing all aspects of the data presented here, including both the decrease of $R_{log,on}$ and the exponential truncation of the probability distributions. While we do not exclude the possibility that there may be some purely mathematical effect behind the decrease in memory, we find the mechanisms tested here to vary in the degree of change in $R_{log,on}$ and, therefore, provide insight into the physical processes behind blinking.

## IV. DISCUSSION

One plausible possibility is to assume that the region of exponential decay of the on-state probability distribution is due to a single rate process. That process can be ionization of the NC, causing a charge to trap externally and the NC to switch from the on- to off-state (alternatives to this assumption are discussed below). In this framework, a large $\tau_c$ value indicates blinking behavior dominated by the distributed kinetics characteristic of a fluctuation-based blinking mechanism. A small $\tau_c$ value indicates behavior dominated by the ionization-based charge trapping process mechanism. The ionization process is not due to slow fluctuations and therefore has little or no correlation with previous events. An increased contribution of the ionization-based charge trapping process to the blinking behavior would therefore cause subsequent on-state durations to become less correlated as $\tau_c$ decreases.

Alternative explanations that do not rely on an additional photoionization process are also considered. Several diffusion-based blinking mechanisms have previously been reported to yield exponentially truncated power law decays for the on duration probability distributions.[14,15,17] These mechanisms do not require the addition of a single rate charge trapping process, and the crossover time is typically related to the rate of diffusion. Additionally, if the slow nature of the fluctuations of the diffusing coordinate is thought to cause the correlations between subsequent on durations, then it is reasonable that increasing the rate of fluctuations may also decrease the correlation. Therefore, an alternative explanation for the $\tau_c$ dependence of $R_{log,on}$ is that increasing the rate of fluctuation in a diffusion-based blinking mechanism will decrease both $\tau_c$ and $R_{log,on}$.

Below, Monte Carlo simulations are employed to generate blinking traces in the framework of two mechanisms. One tests the effect of increased fluctuation rates of a diffusion-based mechanism only. The other tests the possibility that the decrease of $R_{log,on}$ with $\tau_c$ indicates an additional contribution of a single rate charge trapping process to the diffusion-based blinking. The simulated blinking traces are processed by the same analysis methods as used on the experimental data in order to be compared to the results presented in Figure 2b.

**Diffusion-Based Blinking with Variable Fluctuation Rate.** To our knowledge, one mechanism has been shown in the literature to produce blinking traces with correlated subsequent on durations, and we choose this mechanism as the starting point for both simulations to produce the power law distributed blinking behavior. The multiple recombination centers (MRC) mechanism of Frantsuzov et al. proposes hole


dx.doi.org/10.1021/jp3041549 | J. Phys. Chem. B 2013, 117, 4241−4248

trapping at one of $N$ quencher sites on the nanocrystal surface as the nonradiative exciton decay pathway occurring during the off-state.[17] Distributed kinetics, and therefore power law probability distributions, is achieved in this model by time-dependent fluctuations of the hole trapping rate, $k_{trap}(t)$. An illustration of this mechanism is shown in Figure 3a. During an off-state, the hole trapping rate is fast and the QD cycles through three steps: exciton generation, hole trapping, and finally nonradiative recombination of the electron and trapped hole (as shown in Figure 3a). During an on-state, the hole trapping rate is slow and the NC cycles though exciton generation and fluorescent recombination. The MRC mechanism has also been shown to reproduce the memory effects observed experimentally, which the authors attribute to the structured hierarchy of trapping site activation/deactivation rates.[21]

Here we test the effect of increasing the fluctuation rate of a diffusion-based blinking mechanism by Monte Carlo simulations of single NC blinking according to the MRC mechanism. Each simulation reproduces the equations described in refs 17 and 21; however, for this work, the speed of $k_{trap}$ fluctuation is increased by shifting the distribution of activation/deactivation rates of surface trapping sites to higher values.

The fluorescence quantum yield (QY) is calculated as QY = $k_{rad}/(k_{rad} + k_{nrad})$, where the fluorescence decay rate is $k_{rad}$ = $3.33 \times 10^7$ $s^{-1}$ and the nonradiative decay rate is $k_{nrad} = k_{trap}(t)$. The QY is calculated in time steps at least 10 times shorter than the fastest possible $k_{trap}$ fluctuation, such that it can be considered constant within each step. The value of $k_{trap}$ and the configuration of each of 10 trapping sites are re-evaluated at each step according to the equations in references 17 and 21 and in the Supporting Information of this work. Here, the speed of $k_{trap}$ fluctuations is systematically varied by changing the distribution of activation/deactivation rates of the trapping sites. This is achieved by variation of the switching rate of the fastest trapping site ($\gamma_1$). This also affects the switching rates of each of the other slower trapping sites, as they are structured to be interdependent. The full range of activation/deactivation rates for the 10 trapping sites will always span 4.5 orders of magnitude, starting from the rate determined by setting $\gamma_1$ (see the Supporting Information of this work and ref 17 for further details). The QY data are binned in 10 ms durations to produce the blinking trace.

Five 10 min blinking traces are simulated for each variation of the $k_{trap}$ fluctuation speed (each $\gamma_1$ value), and all are processed to be consistent with the experimental data analysis. On duration probability distributions are generated from all on-state events with a given $\gamma_1$ value and are fit using eq 1. Figure 3b illustrates how increasing the rate of $k_{trap}$ fluctuations leads to truncation of the power law probability distributions. $R_{log,on}$ is also calculated for each blinking trace (for a given $\gamma_1$ value), which are averaged and plotted as a function of $\tau_c$ in Figure 3c, where each simulated data point represents a different $\gamma_1$ value. [The authors of ref 17 found that the simulated blinking trace must by at least a factor of 10 longer than the time-scale of the trapping site with the slowest switching rate. Therefore, blinking traces were simulated for 10 000 s (opposed to 600 s) for the case of $1/\gamma_1$ = 10 ms.]

We find that increasing the rate of $k_{trap}$ fluctuations leads to smaller $R_{log,on}$ values, qualitatively similar to the experimental data. However, $R_{log,on}$ is found to increase continuously with $\tau_c$ and the saturation behavior observed experimentally is not

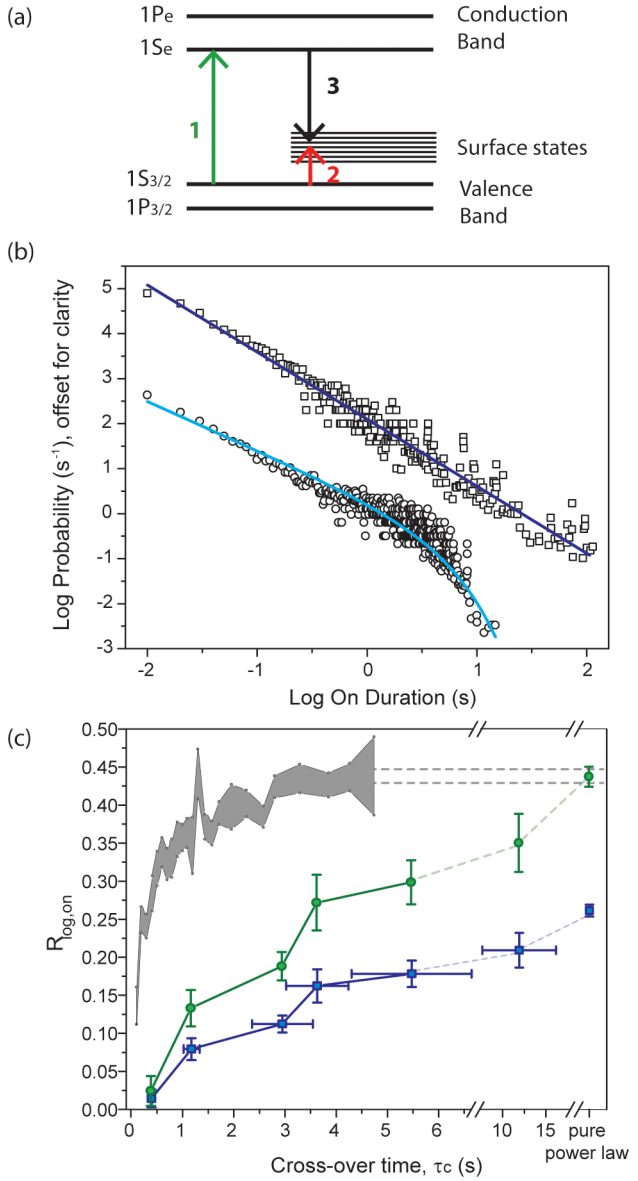


**Figure 3.** Simulated blinking data based on the MRC mechanism[17] with systematic variation of the speed of trapping rate fluctuations. (a) The cycle of exciton generation (1), hole trapping (2), and nonradiative recombination of the electron and trapped hole (3) is thought to occur when $k_{trap}$ is greater than the fluorescence rate. (b) On-state probability distributions for the simulated data are fit to $P(\text{on}) \propto \tau_{on}^{-1.49\pm0.03}$ for slow fluctuations ($1/\gamma_1$ = 10 ms, squares) and to eq 1 with $\tau_c = 3.6 \pm 0.6$ s and $\alpha_{on} = 1.09 \pm 0.07$ for fast fluctuations ($1/\gamma_1$ = 30 $\mu$s, circles). Solid lines indicate the fits. (c) Simulated data (blue squares), normalized simulated data (green circles, normalized such that the maximum $R_{log,on}$ value equals the experimentally observed saturation value), and the full range of experimental data plus and minus error bars (gray shaded area) are overlaid. Each simulated data point represents a different speed of $k_{trap}$ fluctuation (different $\gamma_1$ value), and the final point indicates $R_{log,on}$ for the pure power law distributed data. Dashed gray lines indicate the saturation value of $R_{log,on}$, averaged from all experimental data with $\tau_c > 5.0$ s, plus and minus error bars. All experimental data and error bars are the same as reported in Figure 2b.

reproduced by this model. The slowest $k_{trap}$ fluctuations used here ($1/\gamma_1$ = 10 ms) lead to purely power law distributed on-state probability distributions (Figure 3b, squares) and a maximum of $R_{log,on} = 0.262 \pm 0.008$. To facilitate comparison of


dx.doi.org/10.1021/jp3041549 | J. Phys. Chem. B 2013, 117, 4241−4248

the simulated and experimental data, the simulated $R_{log,on}$ values are normalized such that the maximum value is equal to the saturation value of $R_{log,on}$ observed experimentally. From this comparison, it is apparent that the continuous decrease in $R_{log,on}$ with decreasing $\tau_c$ leads to considerably smaller $R_{log,on}$ values than those measured experimentally. For example, setting $1/\gamma_1 = 30\ \mu s$ generates blinking traces with $\tau_c = 3.6 \pm 0.6$ (Figure 3b, circles) and $R_{log,on} = 0.16 \pm 0.02$. This represents a nearly 38% decrease in $R_{log,on}$ compared to the maximum simulated value, which is inconsistent with the saturation of $R_{log,on}$ for all $\tau_c$ values greater than ~3 s. Overall, we find this explanation of increased $k_{trap}$ fluctuations linking the $R_{log,on}$ and $\tau_c$ decrease is insufficient to reproduce the experimental data.

**Additional Ionization-Induced Trapping Pathway.** The other possibility that the truncation of the on-state probability distributions and decreased on-state memory are due to an additional single rate charge trapping process is now considered. This process is assumed to involve high energy charge trapping sites external to the NC and is illustrated in Figure 4a. Process 1 (green arrow) shows the photogeneration of an electron−hole pair. Ionization of the electron to a distribution of higher energy trapping sites located in the NC environment occurs with the rate $k_{ionize}$ (process 2, red arrow). The ionization mechanism can vary depending on the excitation conditions. Several ionization pathways and experimental evidence for each are discussed below. Process 3 (black arrow) shows the recombination of the trapped electron and hole, which occurs by a distribution of rates according to the distribution of external trapping sites. Including a distribution of high energy trapping sites allows for the off-state duration probability distribution to remain power law distributed, while the on-state distribution crosses over to exponential decay according to $k_{ionize}$. If recombination of the externally trapped electron and hole has not occurred before subsequent absorption events, the newly generated excitons can decay by energy transfer to the lone charge that remains in the QD core (Auger recombination). This model is consistent with several recent publications suggesting that Auger recombination is not the nonradiative decay mechanism of the off-state,[10−12] as it requires Auger recombination to occur only during the fraction of the off events initiated by ionization to external trapping sites.

A secondary photoionization process to switch the NC from the on- to off-state was first suggested by Shimizu et al. to explain the exponential truncation of the on-state power law probability distributions.[9] Photoassisted Auger ionization was initially suggested as the charge ejecting mechanism, and the trap states accessed by ionization were postulated to be on the outer surface of the NC. Several excitation intensity dependent blinking experiments support a photoionization induced trapping mechanism.[25−27]

Alternative ionization mechanisms, such as the self-trapping of a hot electron, have also been suggested to access external charge trapping sites. Excitation wavelength dependent blinking experiments found an energetic threshold to direct trapping of a hot electron for CdSe nanorods approximately 240 meV above the bandgap.[24] Recent work from Galland et al. also reports evidence for the self-trapping of a hot electron, although in this case the trapping sites are found to be energetically located within the band gap of the QD.[28] In both studies, the authors conclude that hot electron trapping occurs in external trapping sites.

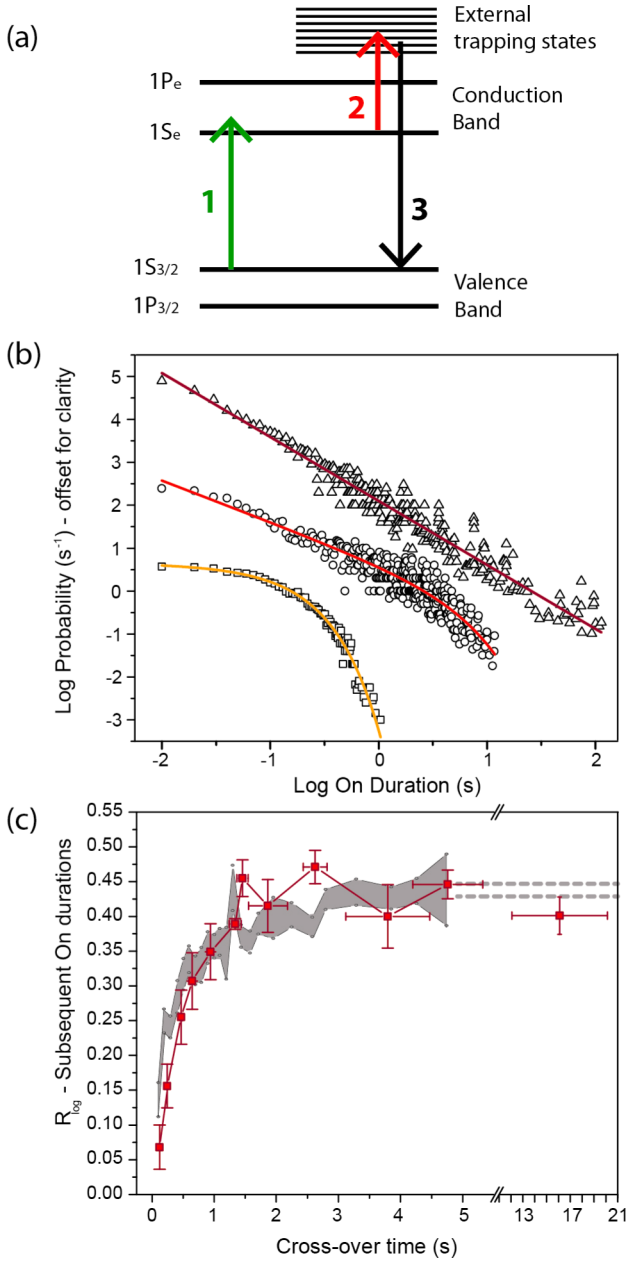


**Figure 4.** The combined effects of a diffusion-based and ionization-induced charge trapping process are modeled with systematic variation of the ionization rate. (a) Illustration of the ionization-induced trapping mechanism: exciton generation (1), ionization of the electron to high energy external trapping sites (2), recombination of the trapped electron and hole (3). (b) On-state probability distributions are shown for three values of $k_{ionize}$: 0 $s^{-1}$ (triangles), 0.5 $s^{-1}$ (circles), and 10 $s^{-1}$ (squares). Fits to eq 1 (solid lines) yield $\tau_c = 4.8 \pm 0.6$ s, $\alpha_{on} = 0.97 \pm 0.04$ ($k_{ionize} = 0.5\ s^{-1}$) and $\tau_c = 0.114 \pm 0.002$ s, $\alpha_{on} = 0.04 \pm 0.03$ ($k_{ionize} = 10\ s^{-1}$). The data set with $k_{ionize} = 0\ s^{-1}$ is fit to $P(on) \propto \tau_{on}^{-1.49\pm0.03}$. (c) Simulated data (red triangles) and the full range of experimental data and error bars (gray shaded area) are overlaid. The error bars are the same as those in Figure 2b. Each simulated data point represents a different $k_{ionize}$ value.

Here we model blinking due to the combined effect of the single rate (ionization) and distributed charge trapping processes, with systematic variation of the ionization rate. The MRC model is again used to simulate blinking behavior with distributed kinetics, resulting in power law on duration


dx.doi.org/10.1021/jp3041549 | J. Phys. Chem. B 2013, 117, 4241−4248

probability distributions and on-state memory. In this case, the model described in the previous section is modified such that the speed of the $k_{trap}$ fluctuations is fixed by setting $1/\gamma_1$ = 10 ms, which produces simulated data with the power law on state probability distribution shown in Figure 4b (triangles). It is also modified such that the occurrence of an external charge trapping event, occurring with the rate $k_{ionize}$, is tested at each time step. In the ionized state, the $k_{trap}$ fluctuations are allowed to continue; however, the fluorescence QY is held constant at a low value with $k_{nrad}$ equal to the Auger recombination rate ($1.0 \times 10^{10}$ $s^{-1}$). Recombination of the externally trapped electron and hole occurs by a distribution of rates given by $k_{detrap} = \kappa_{detrap} \mathrm{Exp}(-x)$, where $x$ is randomly chosen from an exponential distribution of values after each ionization event. $\kappa_{detrap}$ is set to 100 $s^{-1}$, which sets the lower limit to the recombination lifetime of the externally trapped charge at 10 ms (the smallest experimental bin time). The use of larger $\kappa_{detrap}$ values was not found to affect the on-state $\tau_c$ or $R_{log,on}$ values. The maximum lifetime of the ionization-induced trapped charge was limited to 100 s (approximately consistent with the experimentally observed value). Upon recombination, the QY is again calculated using $k_{nrad} = k_{trap}$, where $k_{trap}$ is determined again by the fluctuation-based model. This simulation results in blinking behavior dictated by the $k_{trap}$ fluctuations, interrupted by ionization-induced off state durations. The contribution of the external trapping model is increased through the use of larger $k_{ionize}$ values, thus increasing the frequency of external trapping events.

Five 10 min blinking traces are simulated for each $k_{ionize}$ value and processed to be consistent with the experimental data analysis. We find that the addition of the ionization-induced charge trapping mechanism increases the maximum $R_{log,on}$ value, possibly due to the build-up of on-state durations at the long-time limit imposed by the ionization process. Furthermore, increasing the contribution of the single rate external trapping process (by increasing $k_{ionize}$) induces exponential decay of the long on duration probabilities, such that the data can be fit to eq 1 (see Figure 4b). On-state memory effects are analyzed for the simulated data, and $R_{log,on}$ is also observed to decrease with increasing $k_{ionize}$. For example, Figure 4b shows on-state probability distributions for blinking traces with $k_{ionize}$ = 0.5 $s^{-1}$ (circles) and $k_{ionize}$ = 10 $s^{-1}$ (squares). Note that $\tau_c$ decreases from 4.8 ± 0.6 to 0.114 ± 0.002 s and $R_{log,on}$ decreases from 0.45 ± 0.02 to 0.07 ± 0.03 as $k_{ionize}$ increases from 0.5 to 10 $s^{-1}$.

The average $R_{log,on}$ values are plotted as a function of $\tau_c$ in Figure 4c, where each data point represents a different $k_{ionize}$ value. By overlaying the simulated and experimental data, it is apparent that this mechanism can yield a strong qualitative description of the decrease in $R_{log,on}$ with decreasing $\tau_c$, including the saturation at $R_{log,on}$ at a maximum value for $\tau_c$ > 3 s. From this comparison, we conclude that the experimental data are in support of the combined effect of the two charge trapping mechanisms modeled here. In this framework, the large range of experimentally observed $\tau_c$ and $R_{log,on}$ values reported here are due to varied contributions of a single-rate charge trapping mechanism. For example, higher energy or intensity excitation or an increased number of trapping sites (as suggested for the nanorod morphology) may increase the relative contribution of this additional trapping process.

## V. CONCLUSIONS

In this work, the link between power law distributed blinking dynamics and memory effects is investigated. Employing a variety of sample composition and morphologies, under varied excitation conditions, blinking statistics are measured to have on-state duration probability distributions with $\tau_c$ values ranging from 100 ms to tens of seconds. On-state memory effects are also quantified by the correlation coefficient of subsequent on durations ($R_{log,on}$). A strong correlation is observed between the degree of on-state memory and truncation of the on-state probability distribution. Comparison with simulated blinking data indicates that the correlation of $R_{log,on}$ with the decay of the on duration probability distribution is due to the combined effect of two charge trapping mechanisms that lead to switching between the on- and off-states. NCs that blink with a high degree of on-state memory are dominated by the power law distributed behavior associated with a fluctuation-based charge trapping mechanism. Those with decreased on-state memory are found to have a more significant contribution of exponentially distributed blinking behavior, which is associated with a single-rate charge trapping process.

Blinking data is simulated with power law on-state probability distributions and a high degree of on-state memory using the multiple recombination centers (MRC) mechanism.[17] Increasing the relative contribution of a second, ionization induced charge trapping mechanism is found to induce truncation in the on-duration probability distributions. As the ionization rate increases, the on-state memory is also found to decrease. The ionization induced trapping is assumed to occur by either a multiexciton Auger process or by direct trapping of a hot electron to external high energy charge trapping sites, consistent with the literature.

## ■ ASSOCIATED CONTENT

### Supporting Information

A full list of relevant equations and constants used to reproduce blinking simulations in the context of the multiple recombination centers mechanism of ref 17. This material is available free of charge via the Internet at http://pubs.acs.org.

## ■ AUTHOR INFORMATION

### Corresponding Author

*Phone: 510-643-5467. Fax: 510-643-1376. E-mail: srl@berkeley.edu.

### Notes

The authors declare no competing financial interest.

## ■ ACKNOWLEDGMENTS

The authors gratefully acknowledge financial support by the Director, Office of Science, Office of Basic Energy Sciences, U.S. Department of Energy under Contract No. DE-AC02-05CH11231 through the Materials Research Division.

## ■ REFERENCES

(1) Nirmal, M.; Dabbousi, B. O.; Bawendi, M. G.; Macklin, J. J.; Trautman, J. K.; Harris, T. D.; Brus, L. E. *Nature* **1996**, *383*, 802−804.
(2) Peterson, J. J.; Krauss, T. D. *Nano Lett.* **2006**, *6*, 510−514.
(3) Cichos, F.; Martin, J.; von Borczyskowski, C. *Phys. Rev. B* **2004**, *70*, 115314.
(4) Kuno, M.; Fromm, D. P.; Gallagher, A.; Nesbitt, D.; Micic, O. I.; Nozik, A. J. *Nano Lett.* **2001**, *1*, 557−564.

(5) Wang, S.; Querner, C.; Emmons, T.; Drndic, M.; Crouch, C. H. *J. Phys. Chem. B* **2006**, *110*, 23221−23227.
(6) Glennon, J. J.; Tang, R.; Buhro, W. E.; Loomis, R. A. *Nano Lett.* **2007**, *7*, 3290−3295.
(7) Efros, A. L.; Rosen, M. *Phys. Rev. Lett.* **1997**, *78*, 1110−1113.
(8) Kuno, M.; Fromm, D. P.; Hamann, H. F.; Gallagher, A.; Nesbitt, D. J. *J. Chem. Phys.* **2000**, *112*, 3117−3120.
(9) Shimizu, K. T.; Neuhauser, R. G.; Leatherdale, C. A.; Empedocles, S. A.; Woo, W. K.; Bawendi, M. G. *Phys. Rev. B* **2001**, *63*, 205316.
(10) Zhao, J.; Nair, G.; Fisher, B. R.; Bawendi, M. G. *Phys. Rev. Lett.* **2010**, *104*, 157403.
(11) Rosen, S.; Schwartz, O.; Oron, D. *Phys. Rev. Lett.* **2010**, *104*, 157404.
(12) Cordones, A. A.; Bixby, T. J.; Leone, S. R. *Nano Lett.* **2011**, *11*, 3366−3369.
(13) Califano, M. *J. Phys. Chem. C* **2011**, *115*, 18051−18054.
(14) Tang, J.; Marcus, R. A. *J. Chem. Phys.* **2005**, *123*, 054704.
(15) Frantsuzov, P. A.; Marcus, R. A. *Phys. Rev. B* **2005**, *72*, 155321.
(16) Voznyy, O. *J. Phys. Chem. C* **2011**, *115*, 15927−15932.
(17) Frantsuzov, P. A.; Volkán-Kacsó, S.; Jankó, B. *Phys. Rev. Lett.* **2009**, *103*, 207402.
(18) Zhang, K.; Chang, H.; Fu, A.; Alivisatos, A. P.; Yang, H. *Nano Lett.* **2006**, *6*, 843−847.
(19) Kuno, M.; Fromm, D. P.; Hamann, H. F.; Gallagher, A.; Nesbitt, D. J. *J. Chem. Phys.* **2001**, *115*, 1028−1039.
(20) Stefani, F. D.; Zhong, X.; Knoll, W.; Han, M.; Kreiter, M. *New J. Phys.* **2005**, *7*, 197.
(21) Volkán-Kacsó, S.; Frantsuzov, P. A.; Jankó, B. *Nano Lett.* **2010**, *10*, 2761−2765.
(22) Lu, H. P.; Xun, L.; Xie, X. S. *Science* **1998**, *282*, 1877−1882.
(23) Yu, W. W.; Qu, L.; Guo, W.; Peng, X. *Chem. Mater.* **2003**, *15*, 2854−2860.
(24) Kenneth, L.; Knappenberger, J.; Wong, D. B.; Xu, W.; Schwartzberg, A. M.; Wolcott, A.; Zhang, J. Z.; Leone, S. R. *ACS Nano* **2008**, *2*, 2143−2153.
(25) Cordones, A. A.; Bixby, T. J.; Leone, S. R. *J. Phys. Chem. C* **2011**, *115*, 6341−6349.
(26) Stefani, F. D.; Knoll, W.; Kreiter, M.; Zhong, X.; Han, M. Y. *Phys. Rev. B* **2005**, *72*, 125304.
(27) Peterson, J. J.; Nesbitt, D. J. *Nano Lett.* **2009**, 9.
(28) Galland, C.; Ghosh, Y.; Steinbrück, A.; Sykora, M.; Hollingsworth, J. A.; Klimov, V. I.; Htoon, H. *Nature* **2011**, *479*, 203−208.